Flexocoupling impact on the generalized susceptibility and soft phonon modes in the ordered phase of ferroics

Anna N. Morozovska, Yulian M. Vysochanskii, Oleksandr V. Varenyk, Maxim V. Silibin, Sergei V. Kalinin, and Eugene A. Eliseev

Phys. Rev. B **92**, 094308 — Published 29 September 2015

DOI: 10.1103/PhysRevB.92.094308

To be submitted to Phys.Rev.B.

Flexocoupling impact on the generalized susceptibility and soft phonon modes in the ordered phase of ferroics

Anna N. Morozovska[1*], Yulian M. Vysochanskii[2], Oleksandr V. Varenyk[1], Maxim V. Silibin[3], Sergei V. Kalinin[4], and Eugene A. Eliseev[5†]

[1] Institute of Physics, National Academy of Science of Ukraine,
46, pr. Nauky, 03028 Kyiv, Ukraine
[2] Institute of Solid State Physics and Chemistry, Uzhgorod University,
88000 Uzhgorod, Ukraine
[3]National Research University of Electronic Technology "MIET", Bld. 1, Shokin Square,
124498 Moscow, Russia
[4] The Center for Nanophase Materials Sciences, Oak Ridge National Laboratory,
Oak Ridge, TN 37831
[5] Institute for Problems of Materials Science, National Academy of Science of Ukraine,
3, Krjijanovskogo, 03142 Kyiv, Ukraine

Abstract

Flexoelectric effect impact on the generalized susceptibility and soft phonons dispersion was not studied in the long-range ordered phases of ferroics. Within Landau-Ginzburg-Devonshire approach we obtained analytical expressions for the generalized susceptibility and phonon dispersion relations in the ferroelectric phase. The joint action of static and dynamic flexoelectric effect induces non-diagonal components of generalized susceptibility, which amplitude is proportional to the convolution of the spontaneous polarization with flexocoupling constants. The flexocoupling essentially broadens the k-spectrum of generalized susceptibility and leads to the additional "pushing away" of the optical and acoustic soft mode phonon branches. The degeneration of the transverse optic and acoustic modes disappears in the ferroelectric phase in comparison with the paraelectric phase due to the joint action of flexoelectric coupling and ferroelectric nonlinearity. Obtained results can be principally important for the theoretical analyses of the experimental data broad spectrum including neutron and Brillouin scattering.

[*] Corresponding author 1: anna.n.morozovska@gmail.com

[†] Corresponding author 2: eugene.a.eliseev@gmail.com

I. Introduction

It is difficult to overestimate the significance of the flexoelectric phenomena contribution to the electromechanics of meso- and especially nanoscale objects, for which the strong strain gradients are inevitable present at the surfaces, interfaces, around point and topological defects [1, 2, 3]. According to experiments and Ginzburg-Landau-type theories, flexoelectricity should strongly influence on the broad spectrum of local electromechanical response of the spatially-inhomogeneous systems with inherent strain and/or polarization gradients. There are flexoelectricity-driven imprint [4, 5, 6] and internal bias in thin films [7, 8], spontaneous flexoelectric effect in nanoferroics [9], dead layer effect on ferroelectric thin films conditioned by flexoelectricity [10, 11]. Flexoelectric coupling strongly changes the structural, energetic and electro-transport properties of the domain walls and interfaces in ferroelectrics [12, 13, 14, 15, 16] and ferroelastics [17, 18, 19], leads to the noticeable hardening of ferroelectrics at nano-indentation [20, 21, 22], significantly affects on the local electrochemical strains appeared in response to the excitation of materials with mobile charges by strongly inhomogeneous electric field of the atomic force microscope tip [23, 24] as well as on the mechanical writing of ferroelectric polarization by the tip [25]. Notably, flexoelectricity is allowed by symmetry in any material, making the effect widespread and attractive for advanced applications.

Following a classical definition, the static flexoelectric effect is the response of electric polarization to an elastic strain gradient (direct effect), and, vice versa, the polarization appeared as a response to the strain gradient (inverse effect) [7, 26, 27, 28]. The induced strain is linearly proportional to the polarization gradient $u_{ij}^{sf} = -f_{ijkl}\frac{\partial P_k}{\partial x_l}$, here f_{ijkl} are the components of flexocoupling tensor [1-3], P_k are polarization components. While the static bulk flexoelectric effect can be viewed as an analogue of the piezoelectric effect, the dynamic flexoelectric effect, firstly introduced by Tagantsev as $P_i^{df} = -M_{ij}\frac{\partial^2 U_j}{\partial t^2}$, where U_j is an elastic displacement and M_{ij} is a flexodynamic tensor, has no such analogue, because it corresponds to the polarization response to accelerated motion of the medium in the time domain [1].

Despite the great importance there are only a few ferroics for which the static flexocoupling tensorial coefficients was measured experimentally [29, 30, 31, 32], obtained from early microscopic estimates [27] or recent *ab initio* calculations [33, 34]. The experimental and theoretical results are rather contradictory, indicating on a limited understanding of the effect nature. The situation with dynamic flexocoupling coefficients is even more unclear. Recently, Kvasov and Tagantsev evaluated the strength of the dynamic flexoelectric effect from *ab initio*

calculations and it appeared comparable to that of the static bulk flexoelectric effect [35]. In accordance with this [35] and earlier studies [36, 37] an accurate analysis of the soft phonon spectra extracted from the neutron and Brillouin scattering data can provide information on the components of the total flexocoupling coefficient.

Remarkably that there is an important class of physical problems, for which the impact of flexocoupling can be critically important, but not enough studied, and some aspects are studied rather poorly per se. This is the influence of the static and dynamic flexocouplings on the long-range order parameter fluctuations in the ordered phase of ferroics. Let us underline that the basic experimental methods collecting information about the fluctuations are dynamic dielectric measurements, neutron and Brillouin scattering [38, 39, 40]. Available experimental and theoretical results (see e.g. [41, 42, 43]), mostly demonstrate the significant material-specific impact of the flexocoupling on the scattering spectra. For instance the theory [36-37] predicts a sharp maximum for $SrTiO_3$ in the field dependence of the dielectric loss due to the significant flexoelectric coupling between the soft-mode and acoustic phonon branches, while the analogous field dependence of the loss for $Ba_{0.6}Sr_{0.4}TiO_3$ appeared monotonic because of small flexoelectric coupling.

Flexoelectric effect impact on the generalized susceptibility and soft phonons dispersion was not studied theoretically in the long-range ordered phases of ferroics. The gap in the knowledge motivated us to solve the problem for ferroics with local disordering sources (e.g. chemical strains originated from impurity ions or vacancies).

II. General theory: analytical results near the centre of the Brillouin zone

Generalized expression for the free energy functional has the following form [24]:

$$F = \int_V d^3 r \left(\begin{array}{l} \alpha P_i P_i + \alpha_{ijkl} P_i P_j P_k P_l + \alpha_{ijklmn} P_i P_j P_k P_l P_m P_n + \frac{g_{ijkl}}{2}\left(\frac{\partial P_i}{\partial x_j}\frac{\partial P_k}{\partial x_l}\right) - P_i E_i - q_{ijkl} u_{ij} P_k P_l \\ + \frac{c_{ijkl}}{2} u_{ij} u_{kl} + \frac{f_{ijkm}}{2}\left(u_{ij}\frac{\partial P_m}{\partial x_k} - P_m \frac{\partial u_{ij}}{\partial x_k}\right) + \left(\Xi_{ij}\left(n - n_e\right) + \beta_{ij}\left(N_d^+ - N_{de}^+\right)\right) u_{ij} \end{array} \right) \quad (1)$$

Hereinafter summation is performed over all repeating indexes; P_i is electric polarization. The expansion coefficient α is temperature dependent, $\alpha = \alpha_T\left(T - T_C\right)$, where T is the absolute temperature, T_C is the Curie temperature. Elastic strain tensor is u_{mn}, q_{mnij} is electrostriction tensor, f_{mnli} is the flexoelectric effect tensor. The higher order coefficients α_{ijkl} and α_{ijklmn} are regarded temperature independent; g_{ijkl} are gradient coefficients tensor**,** c_{ijkl} are elastic

compliances. Also we introduce the fluctuations of the electron density, $\delta n(\mathbf{r}) = n(\mathbf{r}) - n_e$, and donor concentration, $\delta N_d(\mathbf{r}) = N_d^+(\mathbf{r}) - N_{de}^+$, from the space charge equilibrium values n_e and N_{de}^+. The electron density in the conduction band is n and N_d^+ is the concentration of ionized donors, e.g. impurity ions or oxygen vacancies. Deformation potential tensor is denoted by Ξ_{ij} and Vegard expansion tensor is β_{ij}.

Dynamic equations of state can be derived from the minimization of Lagrange function, $L = F - T$, where the kinetic energy T is given by expression $T = \frac{\mu}{2}\left(\frac{\partial P_i}{\partial t}\right)^2 + M_{ij}\frac{\partial P_i}{\partial t}\frac{\partial U_j}{\partial t} + \frac{\rho}{2}\left(\frac{\partial U_i}{\partial t}\right)^2$, which includes the dynamic flexoelectric coupling with the tensorial strength M_{ij} [2]. U_i is elastic displacement and ρ is the density of a ferroelectric. Corresponding time-dependent Landau-Ginzburg-Devonshire-type equation of state for ferroelectric polarization reads:

$$\begin{aligned} &\mu\frac{\partial^2 P_i}{\partial t^2} + M_{ij}\frac{\partial^2 U_j}{\partial t^2} + 2\left(\alpha\delta_{ij} - u_{mn}q_{mnij}\right)P_j + 4\alpha_{ijkl}P_jP_kP_l + 6\alpha_{ijklmn}P_jP_kP_lP_mP_n \\ &- g_{ijkl}\frac{\partial^2 P_k}{\partial x_j \partial x_l} = f_{mnli}\frac{\partial u_{mn}}{\partial x_l} + E_i \end{aligned} \tag{2}$$

The total field is the sum of depolarization (*d*) and small probing external (*ext*) fields, $E_i = E_i^d + \delta E_i^{ext}$. The field should be found self-consistently from the electric potential φ as $E_k = -\partial\varphi/\partial x_k$, since the potential satisfy Poisson equation,

$$\varepsilon_b\varepsilon_0\frac{\partial^2\varphi}{\partial x_i^2} = \frac{\partial P_i}{\partial x_i} + e\left(N_d^+ - n\right), \tag{3}$$

where ε_b is background permittivity [44] and ε_0=8.85×10^{-12} F/m is the dielectric permittivity of vacuum, $e\left(N_d^+ - n\right)$ the space charge density, e=1.6×10^{-19} C the electron charge.

Elastic strains u_{ij} and stresses σ_{ij} are related via Generalized Hook law, which include conventional Hook relation, deformation and chemical stresses, flexoelectric and electrostriction terms [23-24]. Since the time-dependent equation of mechanical equilibrium, $\partial\sigma_{ij}/\partial x_j = \rho\partial^2 U_i/\partial t^2$, should be valid, the equation transforms into dynamic Lame-type equation for elastic strain

$$c_{ijkl}\frac{\partial^2 U_l}{\partial x_j \partial x_k} - \rho\frac{\partial^2 U_i}{\partial t^2} - M_{ij}\frac{\partial^2 P_j}{\partial t^2} = -\frac{\partial}{\partial x_j}\left(\Xi_{ij}\delta n + \beta_{ij}\delta N_d + f_{ijkl}\frac{\partial P_l}{\partial x_k} - q_{ijkl}P_kP_l\right). \tag{4}$$

In order to derive expression for the linear generalized susceptibility and correlation function, let us linearize Eqs.(2) for polarization and Eq. (4) for the displacement in the vicinity

of spontaneous values $u_{kl} = u_{kl}^{(s)} + \delta u_{kl}$ and $P_i = P_i^{(s)} + \delta P_i$, where $u_{mn}^{(s)} = s_{mnij} q_{ijkl} P_k^{(s)} P_l^{(s)}$ is the spontaneous strain related to spontaneous polarization $P_l^{(s)}$. Both spontaneous strain and polarization are supposed to be coordinate and time independent in the considered bulk system. Electric field $E_i = E_i^{(s)} + \delta E_i^d + \delta E_i^{ext}$, where depolarization field fluctuations δE_i^d will be estimated in Debye approximation as described in **Appendix A** of **Suppl. Mat** [45]**.**

The Fourier representations in the spatial **k** and frequency ω domain of the linearized solution for polarization and strain fluctuation have the form:

$$\delta\widetilde{P}_j(\mathbf{k},\omega) = \left(\delta\widetilde{E}_i^{ext} + ik_{j'} S_{mi'}(\mathbf{k},\omega)\left(2ik_n q_{mnij} P_j^{(s)} + f_{mnli} k_l k_n - M_{mi}\omega^2\right)\delta\widetilde{C}_{i'j'}\right)\widetilde{\chi}_{ij}(\mathbf{k},\omega), \tag{5a}$$

$$\begin{aligned}\delta\widetilde{U}_k(\mathbf{k},\omega) = {} & -ik_j \delta\widetilde{C}_{ij} S_{ik}(\mathbf{k},\omega) + S_{ik}(\mathbf{k},\omega)\widetilde{\chi}_{sl}(\mathbf{k},\omega)\left(f_{ijml} k_j k_m - M_{il}\omega^2 - 2ik_j q_{ijnl} P_n^{(s)}\right) \\ & \times\left(\delta\widetilde{E}_s^{ext} + i\left(f_{qnps} k_p k_n - M_{qs}\omega^2\right)k_{j'} S_{qi'}(\mathbf{k},\omega)\delta\widetilde{C}_{ij}\right)\end{aligned} \tag{5b}$$

Where $\delta\widetilde{C}_{ij} = \left(\Xi_{ij}\delta\tilde{n} + \beta_{ij}\delta\widetilde{N}_d\right)$. Since the harmonic approach (5) is applicable for small wave vector **k,** we would like to underline that we did not aim to reach the quantitative agreement between the calculated and experimentally observed soft phonon spectra entire the first Brillouin zone. Consideration of the problem for higher **k** values requires including of the anharmonicity and higher gradient terms [46].

Generalized susceptibility, $\widetilde{\chi}_{ij}(\mathbf{k},\omega)$, that is in fact correlation function, and elastic function $S_{ir}(\mathbf{k},\omega)$ included in Eqs.(5) are given by expressions:

$$\widetilde{\chi}_{ij}^{-1}(\mathbf{k},\omega) = \beta_{ij}(\mathbf{k},\omega) + \Theta_{ipjl}(\mathbf{k},\omega) + Q_{ij}(\mathbf{k},\omega) + \gamma_{ijkl}(\mathbf{k},\omega)P_k^{(s)}P_l^{(s)}, \tag{6a}$$

$$S_{ik}^{-1}(\mathbf{k},\omega) = c_{ijkl}k_l k_j - \rho\omega^2\delta_{ik}. \tag{6b}$$

Here the linear dynamic stiffness is affected by depolarization effect as $\beta_{ij}(\mathbf{k},\omega) = \left(2\alpha - \mu\omega^2\right)\delta_{ij} + \dfrac{k_i k_j}{\varepsilon_b\varepsilon_0\left(k^2 + R_d^{-2}\right)}$, where R_d is a Debye screening radius. Nonlinear stiffness $\gamma_{ijkl}(\mathbf{k},\omega) = 12\alpha_{ijkl} - 2q_{mnij}q_{i'j'kl}s_{mni'j'} - 4q_{mnil}q_{i'j'jk}k_{j'}k_n S_{mi'}(\mathbf{k},\omega) + 30\,\alpha_{ijklmn}P_m^{(s)}P_n^{(s)}$. The flexoelectric coupling changes the polarization gradient coefficient tensor g_{ipjl} to the ω and k-dependent tensorial function, that has the following form $\Theta_{ipjl}(\mathbf{k},\omega) = g_{ipjl}k_p k_l - \left(f_{mnli}k_n k_l - M_{mi}\omega^2\right)\left(f_{i'j'pj}k_{j'}k_p - M_{i'j}\omega^2\right)S_{mi'}(\mathbf{k},\omega)$. A new complex term $Q_{ij}(\mathbf{k},\omega)$ is proportional to the convolution of the spontaneous polarization vector with the static and dynamic flexocoupling constants:

$$Q_{ij}(\mathbf{k},\omega) = 2iS_{mi'}(\mathbf{k},\omega)\left(\left(f_{mnpi}k_p k_n - M_{mi}\omega^2\right)k_{j'}q_{i'j'kj} - \left(f_{i'j'pj}k_p k_{j'} - M_{i'j}\omega^2\right)k_n q_{mnik}\right)P_k^{(s)}. \tag{7}$$

Here the static and dynamic flexocoupling appeared in a universal combination $\left(f_{mnpi}k_pk_n - M_{mi}\omega^2\right)$. The term is absent in a paraelectric phase, since there $P_k^{(s)} = 0$.

Note that the Green tensor $\widetilde{\chi}_{ij}(\mathbf{k},\omega)$ is independent on any source of the fluctuations by definition. However polarization variation $\delta\widetilde{P}_j(\mathbf{k},\omega)$ and displacement variation $\delta\widetilde{U}_k(\mathbf{k},\omega)$, which are the solutions of the linearized equations Eqs.(5), are proportional to both sources, external electric field variation $\delta\widetilde{E}_i^{ext}$ and concentration disorder $\delta\widetilde{C}_{ij}$, but the proportionality coefficients are principally different. In particular the relation $\delta\widetilde{P}_j(\mathbf{k},\omega) \sim \delta\widetilde{E}_i^{ext}\widetilde{\chi}_{ij}(\mathbf{k},\omega)$ is conventional and means that the polarization fluctuation is proportional to the dielectric susceptibility, but part proportional to another source $\delta\widetilde{P}_j(\mathbf{k},\omega) \sim ik_{j'}S_{mi'}(\mathbf{k},\omega)\left(2ik_nq_{mnij}P_j^{(s)} + f_{mnli}k_lk_n - M_{mi}\omega^2\right)\widetilde{\chi}_{ij}(\mathbf{k},\omega)\delta\widetilde{C}_{i'j'}$ looks nontrivial due to the presence of additional electrostrictive, static and dynamic flexocoupling contributions $\left(2ik_nq_{mnij}P_j^{(s)} + f_{mnli}k_lk_n - M_{mi}\omega^2\right)$.

Order parameter correlation function is related with the generalized susceptibility via Callen-Welton fluctuation-dissipation theorem [47] and corresponding correlations radius can be determined from the direct matrix $\widetilde{\chi}_{ij}(\mathbf{k},\omega)$.

Following Cochren papers [38], dynamical structural factor of neutron scattering is proportional to the dynamic susceptibility spectra $\widetilde{\chi}(\mathbf{k},\omega)$. Integral intensity of the scattering is proportional to the static spectra, $(d\sigma/d\Omega) \sim \widetilde{\chi}(\mathbf{k},0)$. In the next section we discuss the influence of the flexocoupling on the static spectrum of dielectric susceptibility in a ferroelectric phase.

III. Flexocoupling impact on the dynamic generalized susceptibility in a ferroelectric phase

In general case analytical expressions for $\widetilde{\chi}_{ij}(\mathbf{k},\omega)$ are rather cumbersome. In order to analyze analytically concrete cases, below we consider a uniaxial ferroelectric with a spontaneous polarization directed along z-axes, $\mathbf{P}^{(s)} = (0,0,P_S)$ and other tensorial properties (elastic, electrostrictive and flexoelectric) in the *cubic symmetry approximation*. Analytical results were derived for the basic orientations of the wave vector $\mathbf{k} = (0,0,k_z)$ and $\mathbf{k} = (k_x,0,0)$ (or $\mathbf{k} = (0,k_y,0)$). Calculations details are listed in **Appendix B** of **Suppl. Mat.** [45]. All numerical calculations in this and next sections are performed for $PbZr_{0.4}Ti_{0.6}O_3$ (**PZT**) in its cubic paraelectric and tetragonal ferroelectric phases.

A. Orientation I of the wave vector $\mathbf{k} = (0,0,k_z)$. Ferroelectric phase

For the case, when a wave vector $\mathbf{k}=(0,0,k_z)$ is parallel to the spontaneous polarization direction $\mathbf{P}_S=(0,0,P_S)$, corresponding nonzero components of the susceptibility are [45]:

$$\tilde{\chi}_{11}(\mathbf{k},\omega)=\tilde{\chi}_{22}(\mathbf{k},\omega)=\frac{1}{\alpha_{11}^{*}-\mu\omega^2+g_{44}^{*}k_z^2}. \tag{8a}$$

$$\tilde{\chi}_{33}(\mathbf{k},\omega)=\left(\alpha_{33}^{*}-\mu\omega^2+g_{11}^{*}k_z^2+\frac{k_z^2}{\varepsilon_b\varepsilon_0\left(k_z^2+R_d^{-2}\right)}\right)^{-1}. \tag{8b}$$

Hereinafter the Voight notations are used. The spontaneous polarization contributes to the spectra of $\tilde{\chi}_{ij}(\mathbf{k},\omega)$ via the renormalization of the dielectric stiffness coefficient α as $\alpha_{11}^{*}(\mathbf{k},\omega)=2\alpha+P_S^2\left(\beta_{12}^{*}-\frac{q_{44}^2k_z^2}{c_{44}k^2-\rho\omega^2}\right)+2\alpha_{112}P_S^4$ and $\alpha_{33}^{*}(\mathbf{k},\omega)=2\alpha+P_S^2\left(\beta_{11}^{*}-\frac{4q_{11}^2k_z^2}{c_{11}k_z^2-\rho\omega^2}\right)+30\alpha_{111}P_S^4$. Nonlinear stiffness α_{ijkl} is renormalized by electrostriction coupling as $\beta_{11}^{*}=12\alpha_{11}-\frac{2(q_{11}+2q_{12})^2}{3(c_{11}+2c_{12})}-\frac{2q_{44}^2}{3c_{44}}$ and $\beta_{12}^{*}=2\alpha_{12}-\frac{2(q_{11}+2q_{12})^2}{3(c_{11}+2c_{12})}+\frac{q_{44}^2}{3c_{44}}$. Thus the contribution of spontaneous polarization via ferroelectric nonlinearity ($\sim\beta_{12}^{*}P_S^2$) and electrostriction ($\sim q_{ij}q_{kj}P_S^2$) mechanisms can lead to either increase or decrease of the coefficients α_{ij}^{*} depending on the material constants signs.

Flexocoupling changes the gradient coefficients as

$$g_{11}^{*}(\mathbf{k},\omega)=g_{11}-\frac{\left(f_{11}k_z^2-M_{11}\omega^2\right)^2}{k_z^2\left(c_{11}k_z^2-\rho\omega^2\right)},\qquad g_{44}^{*}(\mathbf{k},\omega)=g_{44}-\frac{\left(f_{44}k_z^2-M_{11}\omega^2\right)^2}{k_z^2\left(c_{44}k_z^2-\rho\omega^2\right)}. \tag{9}$$

The term $(\varepsilon_b\varepsilon_0)^{-1}k_z^2/\left(k_z^2+R_d^{-2}\right)$ in $\tilde{\chi}_{33}$ originates from the depolarization electric field.

The static k-spectra of $\tilde{\chi}_{ij}(\mathbf{k},0)$ calculated in the ferroelectric phase with and without flexocoupling contribution are shown in the **Figure 1a**. The component $\tilde{\chi}_{33}$ is much smaller that the ones due to the depolarization effect. As one can see from the figure flexoelectric effect essentially broadens k-spectrum of all susceptibility components and the broadening increases with k increase. Both spectra coincide in the point **k**=0 as anticipated. The dynamic flexoeffect does not contribute to the spectra in the static case (ω=0). The contribution of spontaneous polarization via ferroelectric nonlinearity and electrostriction mechanisms can lead to both broadening and narrowing on the different components of susceptibility k-spectra.

B. Orientation II of the wave vector $\mathbf{k}=(k_x,0,0)$. Ferroelectric phase

For the **case,** when a fluctuation wave vector $\mathbf{k}=(k_x,0,0)$ is normal to the spontaneous polarization direction $\mathbf{P}_S=(0,0,P_S)$, corresponding nonzero components of the generalized susceptibility are [45]:

$$\tilde{\chi}_{11}(\mathbf{k},\omega)=\frac{\alpha_{11}^*-\mu\omega^2+g_{44}^*k_x^2}{\Delta_{22}(\mathbf{k},\omega)},\qquad \tilde{\chi}_{22}(\mathbf{k},\omega)=\frac{1}{\alpha_{22}^*-\mu\omega^2+g_{44}^*k_x^2}, \tag{10a}$$

$$\tilde{\chi}_{33}(\mathbf{k},\omega)=\left(\alpha_{33}^*-\mu\omega^2+g_{11}^*k_x^2+\frac{k_x^2}{\varepsilon_b\varepsilon_0\left(k_x^2+R_d^{-2}\right)}\right)\frac{1}{\Delta_{22}(\mathbf{k},\omega)}, \tag{10b}$$

$$\tilde{\chi}_{13}(\mathbf{k},\omega)=-\tilde{\chi}_{31}(\mathbf{k},\omega)=\frac{-2iP_S\,k_x}{\Delta_{22}(\mathbf{k},\omega)}\left(\frac{q_{12}\left(f_{11}k_x^2-M_{11}\omega^2\right)}{c_{11}k_x^2-\rho\omega^2}-\frac{q_{44}\left(f_{44}k_x^2-M_{11}\omega^2\right)}{2\left(c_{44}k_x^2-\rho\omega^2\right)}\right). \tag{10c}$$

The spontaneous polarization contributes to the components by the renormalization of the linear dielectric stiffness coefficients $\alpha_{11}^*(\mathbf{k},\omega)=2\alpha+\left(\beta_{11}^*-\frac{4{q_{12}}^2k_x^2}{c_{11}k_x^2-\rho\omega^2}\right)P_S^2+30\alpha_{111}P_S^4$, $\alpha_{22}^*(\mathbf{k},\omega)=2\alpha+\beta_{12}^*P_S^2+2\alpha_{112}P_S^4$ and $\alpha_{33}^*(\mathbf{k},\omega)=2\alpha+\left(\beta_{12}^*-\frac{q_{44}^2k_x^2}{c_{44}k_x^2-\rho\omega^2}\right)P_S^2+2\alpha_{112}P_S^4$. The form of the gradient functions $g_{11}^*(\mathbf{k},\omega)$ and $g_{44}^*(\mathbf{k},\omega)$ used in Eqs.(10) are the same as in the Eq.(9) with the only substitution $k_z\to k_x$. Note that nonzero non-diagonal element $\tilde{\chi}_{13}(\mathbf{k},\omega)$ is proportional to the product of the spontaneous polarization value and flexocoupling constants. Denominator $\Delta_{22}(\mathbf{k},\omega)$ is expressed in terms of inverse matrix elements, $\Delta_{22}(\mathbf{k},\omega)=\tilde{\chi}_{11}^{-1}(\mathbf{k},\omega)\tilde{\chi}_{33}^{-1}(\mathbf{k},\omega)-\tilde{\chi}_{13}^{-1}(\mathbf{k},\omega)\tilde{\chi}_{31}^{-1}(\mathbf{k},\omega)$. The evident expression for $\Delta_{22}(\mathbf{k},\omega)$ is:

$$\begin{aligned}\Delta_{22}(\mathbf{k},\omega)=-4k_x^2P_S^2\left(\frac{q_{12}\left(f_{11}k_x^2-M_{11}\omega^2\right)}{c_{11}k_x^2-\rho\omega^2}-\frac{q_{44}\left(f_{44}k_x^2-M_{11}\omega^2\right)}{2\left(c_{44}k_x^2-\rho\omega^2\right)}\right)^2+\\ \left(\alpha_{11}^*-\mu\omega^2+g_{44}^*k_x^2\right)\left(\alpha_{33}^*-\mu\omega^2+g_{11}^*k_x^2+\frac{k_x^2}{\varepsilon_b\varepsilon_0\left(k_x^2+R_d^{-2}\right)}\right)\end{aligned} \tag{11}$$

The flexocoupling induces several principal changes in the susceptibilities, in particular the terms directly proportional to the product of spontaneous polarization and flexocoupling constants originated from $\tilde{\chi}_{13}(\mathbf{k},\omega)$, as well as to the changes related with the gradient functions $g_{ii}^*(\mathbf{k},\omega)$. The physical interpretation of the susceptibility non-diagonal components given by Eq.(10c) seems very important for us, because it can stimulate the experimental verification of the theoretical prediction. The appearance of $\tilde{\chi}_{13}(\mathbf{k},\omega)=-\tilde{\chi}_{31}(\mathbf{k},\omega)$ in the ferroelectric with noticeable flexocoupling means that the application of the *spatially inhomogeneous* probing electric field in direction 3 (or 1) should induce the polarization change in direction 1 (or 3), that frequency spectrum is proportional to the product of the spontaneous polarization value P_S and

the factors proportional to the static and dynamic flexocoupling constants. We may suggest performing experiments aimed to study the changes of dielectric permittivity tensor non-diagonal components induced by the spatially modulated electromagnetic waves (like induced optical gyration) or electric field gradient in the ferroelectric phase of those ferroics, whose dielectric response to a homogeneous electric field does not contain any non-diagonal contributions.

The static **k**-spectra of $\tilde{\chi}_{ij}(\mathbf{k},0)$ calculated in the ferroelectric phase with and without flexocoupling contribution are shown in the **Figure 1b**. The strict inequalities $\tilde{\chi}_{11} << \tilde{\chi}_{33} << \tilde{\chi}_{22}$ and $\left|\tilde{\chi}_{13}\right| << \tilde{\chi}_{33}$ are valid due to the depolarization effect, because the denominator $\Delta_{22}(\mathbf{k},0)$ includes the depolarization factor $(\varepsilon_b\varepsilon_0)^{-1}k^2/\left(k^2+R_d^{-2}\right)$ and thus strongly decreases $\tilde{\chi}_{11}$, $\tilde{\chi}_{13}$ and $\tilde{\chi}_{33}$ in comparison with the component $\tilde{\chi}_{22}$, which is not affected by depolarizing effect at all as it should be for transverse fluctuations of polarization z-component in the direction 1. Since $\tilde{\chi}_{33}$ contains the depolarization factor in the numerator, it becomes much higher than the components $\tilde{\chi}_{11}$ and $\tilde{\chi}_{13}$. As one can see from the **Figure 1b** flexoelectric effect induces the non-diagonal component $\tilde{\chi}_{13}$, that is odd with respect to **k**, and essentially broadens k-spectrum of the susceptibility diagonal components. The broadening increases with k increase.

C. Paraelectric phase

Finally, let us compare the susceptibility spectrum in ferroelectric and paraelectric phases. Corresponding expressions in the paraelectric phase can be derived from Eqs.(8)-(11) at $\mathbf{P}_S = 0$. Since the determinant $\Delta_{22}(\mathbf{k},\omega) = \left(\alpha_{11}^* - \mu\omega^2 + g_{44}^* k_x^2\right)\left(\alpha_{33}^* - \mu\omega^2 + g_{11}^* k_x^2 + \frac{k_x^2}{\varepsilon_b\varepsilon_0\left(k_x^2 + R_d^{-2}\right)}\right)$ and the susceptibility component $\tilde{\chi}_{13}(\mathbf{k},\omega) = -\tilde{\chi}_{31}(\mathbf{k},\omega) = 0$ in the paraelectric phase, the mathematical form of obtained expressions coincide with Eqs.(8). Thus three diagonal components are nonzero in the paraelectric phase, at that only two of them are different. The static **k**-spectra of $\tilde{\chi}_{ij}(\mathbf{k},0)$ calculated in the paraelectric phase with and without flexocoupling contribution are shown in the **Figure 1c** and **1d** for two different temperatures *T*=750 K **(c)** and *T*=900 K **(d)**. Both paraelectric the spectra look similar to the ferroelectric one calculated for the case $\vec{k} \uparrow\uparrow \vec{P}_S$ and shown in the **Figure 1a.** When the temperature approaches the phase transition at *T*=691 K the maximum height strongly increases for some of the susceptibility components, namely $\tilde{\chi}_{11}(0,k_z) = \tilde{\chi}_{22}(0,k_z)$ increases for the case $\mathbf{k} = (0,0,k_z)$ and

$\tilde{\chi}_{22}(0,k_x)=\tilde{\chi}_{33}(0,k_x)$ increases for the case $\mathbf{k}=(k_x,0,0)$, as anticipated (compare the vertical scale in the **Figure 1c** and **1d**).

The condition of homogeneous distribution instability onset follows from the analyses of the determinant $\det\left[\tilde{\chi}_{ij}^{-1}(\mathbf{k},\omega)\right]=0$. In the static limit (ω=0) and in the paraelectric phase the condition reduces to the following equations:

$$2\alpha c_{44}+k^2\left(c_{44}g_{44}-f_{44}^4\right)=0\,,\qquad \left(2\alpha+\frac{k^2}{\varepsilon_b\varepsilon_0\left(k^2+R_d^{-2}\right)}\right)c_{11}+k^2\left(c_{11}g_{11}-f_{11}^4\right)=0 \qquad (12a)$$

Derivation details of Eq.(12a) are listed in the **Appendix C** of **Suppl. Mat.** [45]. Since the coefficient α is not negative in a paraelectric phase and the factor $\frac{1}{\varepsilon_b\varepsilon_0\left(k_x^2+R_d^{-2}\right)}$ is positive, Eqs.(12a) give the sufficient conditions of the homogeneous distribution stability:

$$f_{11}{}^2<g_{11}c_{11}\,,\qquad f_{44}{}^2<g_{44}c_{44}\,. \qquad (12b)$$

Note, that the condition $f_{44}{}^2<g_{44}c_{44}$ coincides the one derived in Refs. [9, 48]. If one of the inequalities (12b) becomes invalid, one can expect the onset and evolution of the modulated phases.

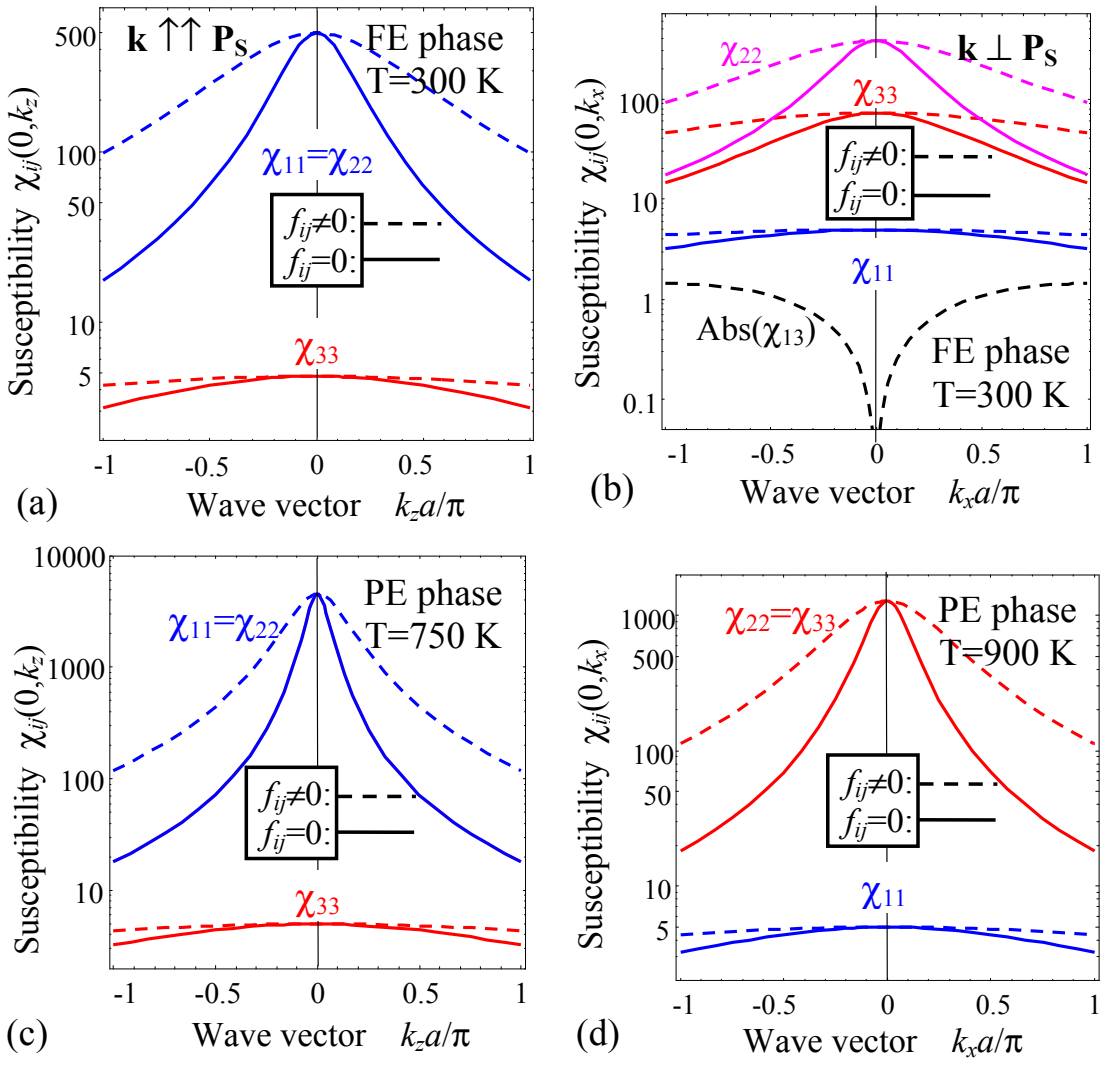

Figure 1. Spatial spectrum of the generalized susceptibility nonzero components $\tilde{\chi}_{ij}(\omega=0,k_x)$ calculated for the different directions fluctuation of the wave vector **k** with respect to the spontaneous polarization $\mathbf{P}_S=(0,0,P_S)$. **(a)** $\vec{k}\uparrow\uparrow\vec{P}_S$ and transverse **(b)** $\vec{k}\perp\vec{P}_S$, a is a lattice constant; temperature T=300 K corresponds to the ferroelectric phase (legend "FE"). Plots **(c,d)** are calculated in paraelectric phase (legend "PE") at temperatures T=750 K **(c)** and T=900 K **(d)**. Dashed curves are calculated with flexoelectric effect (legend "$f_{ij}\neq0$") and solid curves are without it (legend "f_{ij}=0"). The curves are calculated for PZT parameters from the **Table I**.

Correlation radii tensor R_{ij} is proportional to the second derivative of the generalized susceptibility, $R_{ij}^2=-\frac{1}{2\tilde{\chi}_{ij}}\left(\frac{\partial^2\tilde{\chi}_{ij}(\mathbf{k},0)}{\partial k^2}\right)^2\Bigg|_{k\to0}$, where **k** is either k_z or k_x. The dependences of correlation radii of R_{ij} on the flexoelectric coefficients f_{11} and f_{44} are shown in the **Figure 2a** and

2b correspondingly. The correlation radii either monotonically decrease with the flexoelectric coupling constants f_{ij} increase or remained independent on the some f_{ij}. In particular R_{13} always decreases f_{ij} increase, because $\widetilde{\chi}_{13}$ is proportional to f_{ij}. The situation with other R_{ij} depends on the orientation of vector **k** with respect to the spontaneous polarization $\mathbf{P}_S$.

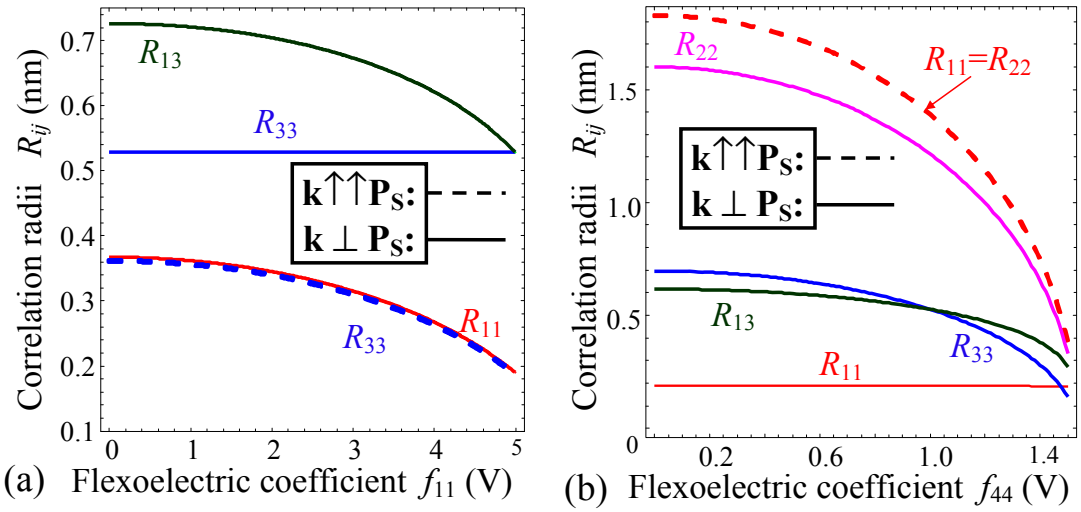

Figure 2. Correlation radii R_{ij} dependence on the flexoelectric coefficient f_{11} **(a)** and f_{44} **(b)**. Dashed curves are calculated for $\vec{k} \uparrow\uparrow \vec{P}_S$ and solid curves correspond to $\vec{k} \perp \vec{P}_S$. The curves are calculated for PZT parameters from the **Table I**. Temperature T=300 K**.**

Table I. Material parameters for bulk ferroelectric

coefficient	**$PbZr_{0.4}Ti_{0.6}O_3$ (from [49, 50,])**	**$PbTiO_3$ (from [51])**
ε_b	5 [44]	5
α_{iT} (×10^5 C^{-2}·mJ/K)	2.12	3.765
T_C (K)	691	752
$\alpha^{(\sigma)}_{ij}$ (×10^8 C^{-4}·m^5J)	a_{11}= 0.3614, a_{12}= 3.233	a_{11}= – 0.725, a_{12}=7.50
α_{ijk} (×10^8 Jm^9C^{-6}·)	a_{111}= 1.859, a_{112}= 8.503 a_{123}= –40.63	a_{111}= 2.606, a_{112}= 6.10, a_{123}= –36.60
q_{ij} (×10^9 V·m/C)	q_{11}=8.91, q_{12}= –0.787, q_{44}=3.18	q_{11}=11, q_{44}=7
c_{ij} (×10^{10} Pa)	c_{11}=17.0, c_{12}= 8.2, c_{44}=4.7	c_{11}=18, c_{12}=7.9, c_{44}=11
g_{ij} (×10^{-10} $C^{-2}m^3$J)	g_{11}=2.0, g_{44}=1.0 * Estimated form domain wall width	g_{11}=1.5, g_{44}=0.5
f_{ij} (V)	f_{11}= 5, f_{12}= – 1, f_{44}= +1 *estimated from [27, 30, 31, 32]	f_{11}= – 8, f_{44}= – 1.9
M_{11} (V s^2/m^2)	6×10^{-8} [35]	– 2×10^{-8}
ρ (×10^3 kg/m^3)	8.087 * *At normal conditions	7.986
μ (×10^{-18} s^2mJ)	1.413 [41]	1.59
R_d (m)	from 20 nm to infinity	infinity

IV. The impact of flexocoupling on soft phonon spectra

Starting from classical Shirane papers [41-43] soft phonon dispersion were studied experimentally for several incipient and proper ferroelectrics. Below we study the impact of the flexocoupling on the soft phonon dispersion in ferroelectric phase and compare the results with a paraelectric phase.

Dispersion relations for longitudinal and transverse optical (LO and TO) and acoustical (LA and TA) modes can be obtained from the analyses of the determinant $\det\left[\tilde{\chi}_{ij}^{-1}(\mathbf{k},\omega)\right]=0$. Dispersion relations for the fluctuation wave vector direction $\mathbf{k}=(0,0,k_z)$ were derived for the cases $\mathbf{k}\uparrow\uparrow\delta P$ and $\mathbf{k}\perp\delta P$ correspondingly. They acquire the form:

$$\left(\begin{array}{l} 2\alpha-\mu\omega^2+g_{11}k_z^2-\dfrac{\left(f_{11}k_z^2-M_{11}\omega^2\right)^2}{c_{11}k_z^2-\rho\omega^2}+\dfrac{k_z^2}{\varepsilon_b\varepsilon_0\left(k_z^2+R_d^{-2}\right)} \\ +P_S^2\left(\beta_{11}^*-\dfrac{4q_{11}^2k_z^2}{c_{11}k_z^2-\rho\omega^2}\right)+30\alpha_{111}P_S^4 \end{array}\right)=0, \qquad (13a)$$

$$2\alpha-\mu\omega^2+g_{44}k_z^2-\frac{\left(f_{44}k_z^2-M_{11}\omega^2\right)^2}{c_{44}k_z^2-\rho\omega^2}+P_S^2\left(\beta_{12}^*-\frac{q_{44}^2k_z^2}{c_{44}k_z^2-\rho\omega^2}\right)+2\alpha_{112}P_S^4=0 \qquad (13b)$$

Dispersion relation for the fluctuation wave vector direction $\mathbf{k}=(k_x,0,0)$ has the form

$$\left(2\alpha-\mu\omega^2+g_{44}^*(\mathbf{k},\omega)k_x^2+P_S^2\beta_{12}^*\right)\Delta_{22}(\mathbf{k},\omega)=0. \qquad (13c)$$

The terms originated from the static and dynamic flexocoupling appeared in the combination $\left(f_{11}k_z^2-M_{11}\omega^2\right)$ and $\left(f_{44}k_z^2-M_{11}\omega^2\right)$ in the equations. The spontaneous polarization P_S via ferroelectric nonlinearity and electrostriction mechanisms generates the term proportional to $\beta_{ij}^*P_S^2$, $\alpha_{ijkl}P_S^4$ and $q_{ij}q_{kj}P_S^2$ in the equations. Due to the k-dependence of the terms $\sim P_S^2$ the analytical solution of Eqs.(13) is absent in a ferroelectric phase.

The features of the soft phonon k-spectra were calculated with static ($f_{ij}\neq0$ and $M_{ij}=0$) and dynamic flexocoupling ($f_{ij}\neq0$ and $M_{ij}\neq0$) and without it ($f_{ij}=0$ and $M_{ij}=0$). Spectra calculated in the paraelectric and ferroelectric phase for the cases $\vec{k}\uparrow\uparrow\vec{P}_S$ and $\vec{k}\perp\vec{P}_S$ are compared in the **Figure 3a, 3b** and **3c** correspondingly. Parameters corresponding to PZT are listed in the **Table I.**

Equations (13) have relatively simple analytical solution in a paraelectric phase ($P_S^2=0$), namely two acoustic (LA and TA) and two optical (LO and TO) modes (see **Figure 3a**). Equation (13a) has an analytical solution in a ferroelectric phase also, and it contains one acoustic mode LA_3 and a very high longitudinal optical mode (LO) with frequency at about $150\times10^{12}s^{-1}$, that is maximal in the dielectric limit ($R_d^{-2}\to0$). The LO-mode is weakly

dependent on temperature due to the depolarization factor $\frac{k_z^2}{\varepsilon_b\varepsilon_0\left(k_z^2+R_d^{-2}\right)}$, that becomes giant in the dielectric limit. Both paraelectric and ferroelectric spectra contain rather high frequency longitudinal optic modes (LO) due to the strong depolarization field that is maximal in the dielectric limit and is almost independent on the flexocouplings and temperature. Therefore the LO modes are not shown in the **Figure 3.** The longitudinal soft mode LA_3 is insensitive to the flexocoupling, because its dispersion is strongly affected by the depolarization effect.

Due to the k-dependence of the terms $\sim P_S^2$ the analytical solution of Eqs.(13b) is absent in a ferroelectric phase. Corresponding numerical solution has four degenerated transverse soft phonon branches, namely two optical ($TO_1 = TO_2$) and two acoustic ($TA_1 = TA_2$) modes (see **Figure 3b**). All the transverse soft modes are relatively sensitive to both dynamic and static flexocoupling constants, especially at $k_z a/\pi \geq 0.03$, a is a lattice constant (compare solid, dotted and dashed curves for TO modes in **Figure 3a** and **3b**). Since the calculated phonon spectrum in the paraelectric phase has two acoustic (LA and TA) and two optical (LO and TO) modes, we can conclude that the appearance of spontaneous polarization does not lead to the qualitative changes in the spectra for the case of wave vector direction $\vec{k} \uparrow\uparrow \vec{P}_S$.

Without flexocoupling the numerical solution of Eq.(13c) has six different phonon branches in the ferroelectric phase for the case $\vec{k} \perp \vec{P}_S$, namely three optical (LO, TO_2 and TO_3) and three acoustic (LA_1, TA_2, TA_3) modes, at that the frequencies of the modes TA_2 and TA_3 are almost the same at $ka_x/\pi < 0.3$ (see solid curves in the **Figure 3c**). With the flexocoupling included, the solution in the ferroelectric phase has also six different soft phonon branches, three optical (LO, TO_2 and TO_3) and three acoustic (LA_1, TA_2 and TA_3) modes, at that the frequencies of the modes TA_2 and TA_3 are noticeably different at $ka_x/\pi < 0.3$ (see dashed and dotted curves in the **Figure 3c**). Since the phonon spectra in the paraelectric phase has two optical (LO and TO) and two acoustic (LA and TA) modes (see **Figure 3a**), we can conclude that the spontaneous polarization appearance leads to the removal of the degeneration of the acoustic and optic modes TA and TO for the case $\vec{k} \perp \vec{P}_S$ and consequently to the appearance of different transverse acoustic and optics modes TA_2 and TA_3, TO_2 and TO_3. The transverse $TO_{2,3}$ and $TA_{2,3}$ modes are relatively sensitive to both static and dynamic flexoelectric coupling strength for the case $\vec{k} \perp \vec{P}_S$ and $k_x a/\pi \geq 0.1$ for acoustic modes and for small k for optic modes correspondingly, meanwhile the longitudinal LA_1 mode becomes sensitive to the coupling at $k_x a/\pi \geq 0.15$ (compare solid, dotted and dashed curves in the **Figure 3c**). The flexoelectric coupling significantly increases the splitting of the TA_2 and TA_3 modes. Moreover, TO_3 and LA_1

modes are "pushed away" by the static and dynamic flexocoupling in the ferroelectric phase at small **k** ($k_x a/\pi \le 0.15$) and start to approach each other at $k_x a/\pi \ge 0.15$ (compare solid and dashed curves inside in the **Figure 3d**). The effects give us the opportunity to define the static and dynamic flexocoupling constants (e.g. f_{11}, f_{44} and M_{11}) from soft phonons spectra in the assumption of other known materials parameters.

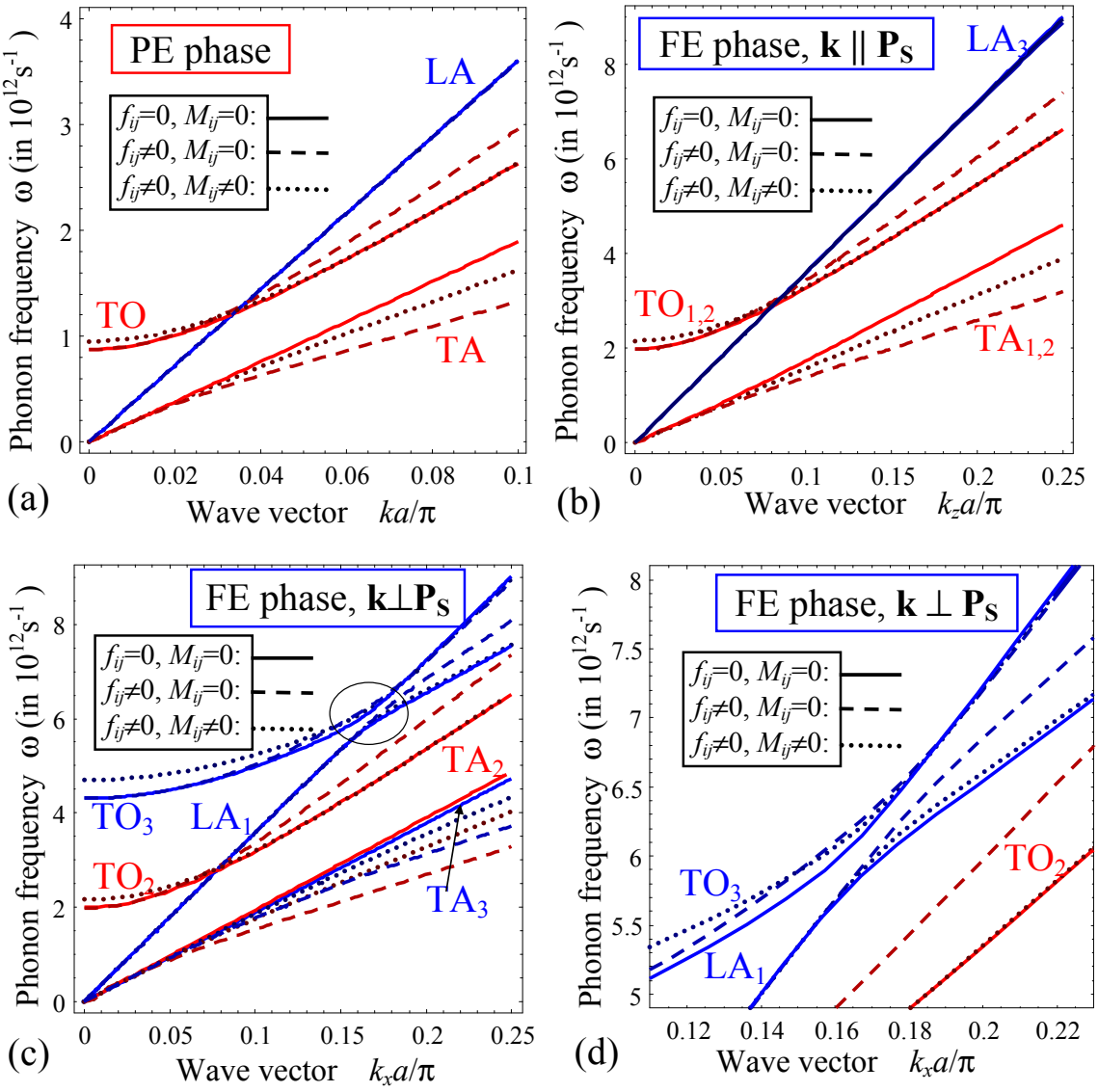

Figure 3. Soft phonon frequency dispersion. The wave vector k is reduced in π/a units, a is a lattice constant. Plot **(a)** corresponds to the paraelectric phase (legend "PE") of PZT at temperature T=700 K, plots **(b)** and **(c)** are calculated in the ferroelectric phase (legend "FE") at temperature T=680 K) for longitudinal $\vec{k} \uparrow\uparrow \vec{P}_S$ **(b)** and transverse $\vec{k} \perp \vec{P}_S$ **(c,d)** fluctuation of the wave vector directions with respect to the spontaneous polarization $\mathbf{P}_S = (0,0,P_S)$. Solid curves are calculated without flexoelectric coupling (legend "f_{ij}=0, M_{ij}=0"); dashed curves are

calculated with the static, but without the dynamic coupling (legend "$f_{ij}\neq 0$, $M_{ij}=0$"); dotted curves are calculated with the dynamic and static flexoelectric couplings included (legend "$f_{ij}\neq 0$, $M_{ij}\neq 0$"). **(d)** Zoom of the plot **(c)** inside the circle. The curves are calculated for PZT parameters from the **Table I**.

Finally, let us answer on the question how important is the flexocoupling for quantitative description of the observed phonon spectra. In the **Figure 4** we compare the paraelectric and ferroelectric soft phonon spectra of $PbTiO_3$ calculated by us with the spectra experimentally observed by Shirane et al [41]**.** Parameters corresponding to the best fitting of $PbTiO_3$ spectra are listed in the last column of the **Table I.** It is clear from the figure that only the solid curves calculated for both nonzero static and dynamic flexocoupling constants ($f_{11}=-8$ V, $f_{44}=-1.9$ V and $M_{11}=-2\times10^{-8}$ V s^2/m^2) describe quantitatively observed paraelectric and ferroelectric soft phonon spectra of $PbTiO_3$ at small **k** (compare dotted, dashed and solid curves in the **Figures 4**). Therefore it is hardly possibly to fit the experimental results without inclusion of nonzero static and dynamic flexocoupling constants. Hence we conclude that both these contributions are critically important to describe quantitatively the available experimental data even at small k.

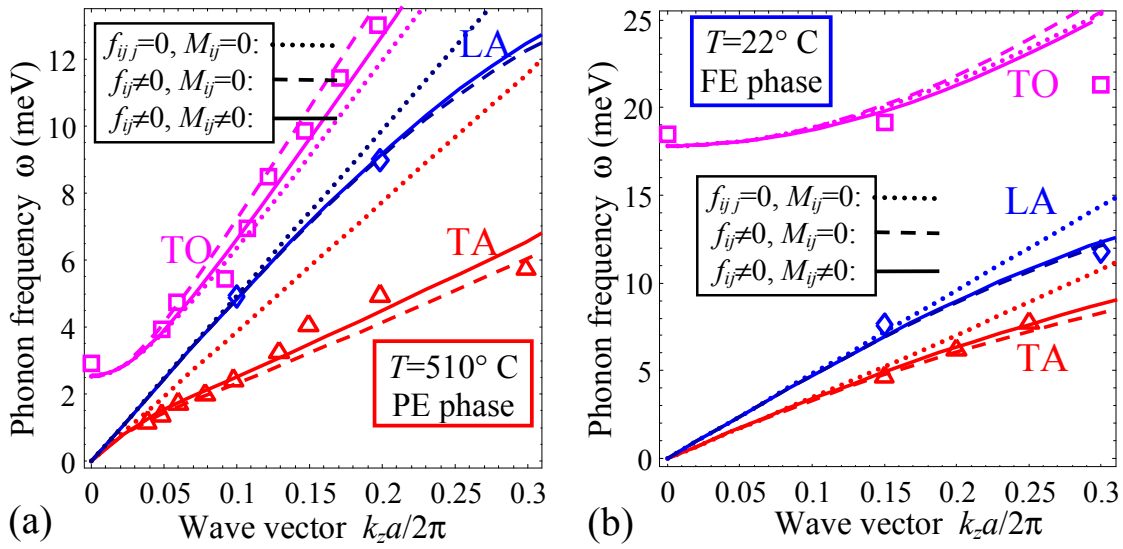

Figure 4. Soft phonon branches frequency vs. k calculated in $PbTiO_3$. Plot **(a)** corresponds to the paraelectric (PE) phase of (T=510 C), plot **(b)** is calculated in the ferroelectric (FE) phase (T=22 C) for the case $\vec{k} \uparrow\uparrow \vec{P}_S$. Symbols are experimental data from ref.[41]. Dotted curves are calculated without flexoelectric coupling (legend "$f_{ij}=0$, $M_{ij}=0$"); dashed curves are calculated with the static but without the dynamic effect (legend "$f_{ij}\neq 0$, $M_{ij}=0$") and solid curves are calculated with the dynamic and static flexoelectric effects included (legend "$f_{ij}\neq 0$, $M_{ij}\neq 0$").

Parameters corresponding to the best fitting of $PbTiO_3$ spectra are listed in the last row of the **Table I.**

VI. Summary

Within Landau-Ginzburg-Devonshire approach we establish the impact of the static and dynamic flexocoupling on the correlation function of the long-range order parameter fluctuations in ferroelectric phase of ferroics with local disordering sources and obtained analytical expressions for the generalized susceptibility and phonon dispersion relations for ferroelectrics with arbitrary symmetry, elastic and electrostrictive anisotropy. Relatively simple analytical expressions for the susceptibility components and soft phonons dispersion law were derived in the cubic approximation for the elastic and electrostrictive properties of ferroelectric. Using the expressions, we studied the physical manifestations of the flexocoupling and lead to the following conclusions:

a) The joint action of static and dynamic flexoelectric effect induces non-diagonal components of generalized susceptibility, which amplitude are proportional to the convolution of the spontaneous polarization with flexocoupling constants.

b) The flexocoupling essentially broadens the k-spectrum of generalized susceptibility and so decreases the correlation radii

c) The contribution of spontaneous polarization via ferroelectric nonlinearity and electrostriction mechanisms can lead to both broadening and narrowing on the susceptibility k-spectrum.

d) The spontaneous polarization appearance leads to the removal of the modes degeneration and consequently to the appearance of different transverse acoustic and optics modes. The flexoelectric coupling significantly increases the splitting of the acoustic modes, as well as it leads to the additional "pushing away" of the optical and acoustic soft mode phonon branches.

e) It appeared hardly possible to fit adequately the experimentally observed phonon spectra of lead zirconate titanate for zero static and dynamic flexocoupling constants even at small k. Hence we conclude that both the static and dynamic contributions are critically important to describe quantitatively the available experimental data.

Also we would like to underline that we did not aim to reach the quantitative agreement between the calculated and experimentally observed soft phonon spectra entire the first Brillouin zone. Consideration of the problem for higher **k** values requires including the anharmonicity and higher gradient terms to modify the harmonic approach we used. However our results prove the evident importance of the static and dynamic flexocouplings for the adequate description of the generalized susceptibilities and soft phonon spectra near the centre of the Brillouin zone. Since

modern and classic experimental methods readily capture the small-k region, further study of the flexocouplings impact on the susceptibility spectra for all crystallographic symmetries seems important. Note, that our model does not contain any damping, but the energy dissipation (e.g. sound attenuation or optic phonons damping [52]) also could be analyzed with account of flexocoupling on base of the Landau-Khalatnikov theory.

Obtained results can be principally important for theoretical analyses of the experimental data broad spectrum including neutron and Brillouin scattering, which collects unique information from the structural factors and phonon dispersion.

Acknowledgements. Authors gratefully acknowledge extremely useful suggestion to include the dynamic flexoelectric coupling into the theoretical consideration, multiple consultations and discussions with Prof. A.K. Tagantsev (EPFL). E.A.E. and A.N.M. acknowledge National Academy of Sciences of Ukraine (grants 35-02-15 and 07-06-15). M.V.S. acknowledge Russian Science Foundation (Grant No. 15-19-20038).

Authors contribution. A.N.M. formulated the theoretical problem, derived general analytical expressions and wrote the initial text of the manuscript with figures. E.A.E. derived the analytical expressions for cubic symmetry, performed corresponding numerical simulations and prepared illustrations jointly with O.V.V. Y.M.V. densely worked on the improvement, physical interpretation and correlation with experiment of the obtained theoretical results. M.V.S. and S.V.K., jointly with A.N.M. and Y.M.V., densely work on the improvement of the paper text, discussion and conclusions.

References

[1] D. Lee, A. Yoon, S.Y. Jang, J.-G. Yoon, J.-S. Chung, M. Kim, J. F. Scott, and T.W. Noh. Giant Flexoelectric Effect in Ferroelectric Epitaxial Thin Films. PRL **107**, 057602 (2011).

[2] P V Yudin and A K Tagantsev. Fundamentals of flexoelectricity in solids. Nanotechnology, 24, 432001 (2013).

[3] P. Zubko, G. Catalan, A.K. Tagantsev. Flexoelectric Effect in Solids. *Annual Review of Materials Research* 43: 387-421. (2013).

[4] Abe, Kazuhide, Shuichi Komatsu, Naoko Yanase, Kenya Sano, and Takashi Kawakubo. "Asymmetric ferroelectricity and anomalous current conduction in heteroepitaxial BaTiO3 thin films." Japanese journal of applied physics 36, no. 9S: 5846 (1997).

[5] K. Abe, N. Yanase, T. Yasumoto, and T. Kawakubo. "Voltage shift phenomena in a heteroepitaxial BaTiO3 thin film capacitor." J. Appl. Phys. 91, no. 1: 323-330 (2002).

[6] Alexander K. Tagantsev, L. Eric Cross, and Jan Fousek. *Domains in Ferroic Crystals and Thin Films*. (Springer New York, 2010)

[7] G. Catalan, L.J. Sinnamon and J.M. Gregg The effect of flexoelectricity on the dielectric properties of inhomogeneously strained ferroelectric thin films J. Phys.: Condens. Matter 16, 2253 (2004).

[8] G. Catalan, Beatriz Noheda, J. McAneney, L. J. Sinnamon, and J. M. Gregg. "Strain gradients in epitaxial ferroelectrics." Phys. Rev. B 72, no. 2: 020102 (2005).

[9] E.A. Eliseev, A.N. Morozovska, M.D. Glinchuk, and R. Blinc. Spontaneous flexoelectric/flexomagnetic effect in nanoferroics. Phys. Rev. B. **79**, № 16, 165433-1-10, (2009).

[10] M. S.Majdoub, R. Maranganti, and P. Sharma. "Understanding the origins of the intrinsic dead layer effect in nanocapacitors." Phys. Rev. *B* 79, no. 11: 115412 (2009).

[11] Hao Zhou, Jiawang Hong, Yihui Zhang, Faxin Li, Yongmao Pei, and Daining Fang. "Flexoelectricity induced increase of critical thickness in epitaxial ferroelectric thin films." Physica B: Condensed Matter 407, no. 17: 3377-3381 (2012).

[12] Peter Maksymovych, Anna N. Morozovska, Pu Yu, Eugene A. Eliseev, Ying-Hao Chu, Ramamoorthy Ramesh, Arthur P. Baddorf, Sergei V. Kalinin. Tunable metallic conductance in ferroelectric nanodomains. Nano Letters **12**, 209–213 (2012).

[13] E.A. Eliseev, A.N. Morozovska, G.S. Svechnikov, Peter Maksymovych, S.V. Kalinin. Domain wall conduction in multiaxial ferroelectrics: impact of the wall tilt, curvature, flexoelectric coupling, electrostriction, proximity and finite size effects. Phys. Rev.B. **85**, 045312 (2012)

[14] Albina Y. Borisevich, E. A. Eliseev, A. N. Morozovska, C-J. Cheng, J-Y. Lin, Ying-Hao Chu, Daisuke Kan, Ichiro Takeuchi, V. Nagarajan, and Sergei V. Kalinin. "Atomic-scale evolution of modulated phases at the ferroelectric–antiferroelectric morphotropic phase boundary controlled by flexoelectric interaction." Nature communications 3: 775 (2012).

[15] P.V. Yudin, , A. K. Tagantsev, E. A. Eliseev, A. N. Morozovska, and Nava Setter. "Bichiral structure of ferroelectric domain walls driven by flexoelectricity." Physical Review B 86, no. 13: 134102 (2012).

[16] Eugene A. Eliseev, Peter V. Yudin, Sergei V. Kalinin, Nava Setter, Alexander K. Tagantsev and Anna N. Morozovska. Structural phase transitions and electronic phenomena at 180-degree domain walls in rhombohedral BaTiO3. Phys.Rev. **B 87**, 054111 (2013).

[17] Anna N.Morozovska, Eugene A. Eliseev, Maya D. Glinchuk, Long-Qing Chen, and Venkatraman Gopalan. "Interfacial polarization and pyroelectricity in antiferrodistortive structures induced by a flexoelectric effect and rotostriction." *Physical Review B* 85, no. 9: 094107 (2012).

[18] Eugene A. Eliseev, Anna N. Morozovska, Yijia Gu, Albina Y. Borisevich, Long-Qing Chen and Venkatraman Gopalan, and Sergei V. Kalinin. Conductivity of twin walls - surface junctions in ferroelastics: interplay of deformation potential, octahedral rotations, improper ferroelectricity and flexoelectric coupling. Phys. Rev. **B 86**, 085416 (2012)

[19] Eugene A. Eliseev, Sergei V. Kalinin, Yijia Gu, Maya D. Glinchuk, Victoria Khist, Albina Borisevich, Venkatraman Gopalan, Long-Qing Chen, and Anna N. Morozovska. Universal emergence of spatially-modulated structures induced by flexo-antiferrodistortive coupling in multiferroics. Phys.Rev. **B 88**, 224105 (2013)

[20] M. Gharbi, Z. H. Sun, P. Sharma, and K. White. "The origins of electromechanical indentation size effect in ferroelectrics." *Applied Physics Letters* 95, no. 14: 142901 (2009).

[21]M. Gharbi, Z. H. Sun, P. Sharma, K. White, and S. El-Borgi. "Flexoelectric properties of ferroelectrics and the nanoindentation size-effect." International Journal of Solids and Structures 48, no. 2: 249-256 (2011).

[22] C. R. Robinson, K. W. White, and P. Sharma. "Elucidating the mechanism for indentation size-effect in dielectrics." Applied Physics Letters 101, no. 12: 2901 (2012).

[23] A.N. Morozovska, E.A. Eliseev, A.K. Tagantsev, S.L. Bravina, Long-Qing Chen, and S.V. Kalinin. Thermodynamics of electromechanically coupled mixed ionic-electronic conductors: Deformation potential, Vegard strains, and flexoelectric effect. Phys. Rev. **B 83**, 195313 (2011).

[24] A.N. Morozovska, E.A. Eliseev, G.S. Svechnikov, and S.V. Kalinin. Nanoscale electromechanics of paraelectric materials with mobile charges: Size effects and nonlinearity of electromechanical response of $SrTiO_3$ films. Phys. Rev. B 84, 045402 (2011).

[25] H. Lu, C.-W. Bark, D. Esque de los Ojos, J. Alcala, C. B. Eom, G. Catalan, A. Gruverman. Mechanical Writing of Ferroelectric Polarization. *Science* 336, 59 (2012)

[26]. V.S. Mashkevich, and K.B. Tolpygo, *Zh.Eksp.Teor.Fiz.* **31**, 520 (1957) [*Sov.Phys. JETP*, **4**, 455 (1957)].

[27] Sh. M. Kogan, " Piezoelectric effect under an inhomogeneous strain and an acoustic scattering of carriers of current in crystals "Solid State Physics, Vol. **5**, 10, 2829 (1963)

[28]. A.K. Tagantsev, "Piezoelectricity and flexoelectricity in crystalline dielectrics." Phys. Rev B, **34**, 5883 (1986)

[29] W. Ma, L.E. Cross. "Strain-gradient-induced electric polarization in lead zirconate titanate ceramics." Applied Physics Letters, 82(19), 3293 (2003).

[30] P. Zubko, G. Catalan, A. Buckley, P.R. L. Welche, J. F. Scott. "Strain-gradient-induced polarization in SrTiO 3 single crystals." Phys. Rev. Lett. **99**, 167601 (2007).

[31] W. Ma and L. E. Cross, "Flexoelectricity of barium titanate." Appl. Phys. Lett., **88**, 232902 (2006).

[32] W. Ma and L. E. Cross, "Flexoelectric effect in ceramic lead zirconate titanate." Appl. Phys. Lett. 86, 072905 (2005).

[33] I. Ponomareva, A. K. Tagantsev, L. Bellaiche. "Finite-temperature flexoelectricity in ferroelectric thin films from first principles." Phys.Rev. B 85, 104101 (2012)

[34] Jiawang Hong and David Vanderbilt. First-principles theory of frozen-ion flexoelectricity. Phys.Rev. B 84, 180101(R) (2011)

[35] Alexander Kvasov, Alexander K. Tagantsev, Dynamic flexoelectric effect in perovskites from first principles calculations, http://arxiv.org/abs/1503.05355

[36] E. Farhi, A.K. Tagantsev, R. Currat, B. Hehlen, E. Courtens, and L.A. Boatner. "Low energy phonon spectrum and its parameterization in pure KTaO3 below 80 K." Eur. Phys. J. B **15**, 615-623 (2000)

[37] K. F. Astafiev, A. K. Tagantsev, and N. Setter. "Quasi-Debye microwave loss as an intrinsic limitation of microwave performance of tunable components based on SrTiO3 and BaxSr1-xTiO3 ferroelectrics." J. Appl. Phys. **97**, 014106 (2005)

[38] W. Cochran. Dynamical, scattering and dielectric properties of ferroelectric crystals, Advances in Physics, 18:72, 157-192 (1969).

[39] J. Hlinka, I. Gregora, and V. Vorlıcek. Complete spectrum of long-wavelength phonon modes in Sn2P2S6 by Raman scattering. Phys.Rev. B **65**, 064308 (2002)

[40] R.M.Yevych, Yu. M. Vysochanskii, M.M. Khoma and S.I. Perechinskii. Lattice instability at phase transitions near the Lifshitz point in proper monoclinic ferroelectricsJ. Phys.: Condens. Matter **18**, 4047–4064 (2006)

[41] G. Shirane, J. D. Axe, J. Harada, and J. P. Remeika. "Soft ferroelectric modes in lead titanate." *Physical Review B* 2, no. 1: 155 (1970)

[42] G. Shirane, J. D. Axe, J. Harada, and A. Linz. "Inelastic Neutron Scattering from Single-Domain $BaTiO_3$. *Physical Review B* 2, no. 9: 3651 (1970).

[43] G. Shirane, B. C. Frazer, V. J. Minkiewicz, J. A. Leake, and A. Linz. "Soft Optic Modes in Barium Titanate" Phys. Rev. Lett. 19, 234 (1967)

[44] A.K. Tagantsev, and G. Gerra, "Interface-induced phenomena in polarization response of ferroelectric thin films." J. Appl. Phys. **100**, 051607 (2006)

[45] Supplementary Materials [URL will be provided by the publisher]

[46] J. D. Freire, and R. S. Katiyar. "Lattice dynamics of crystals with tetragonal BaTiO 3 structure." Physical Review **B 37**, 2074(1988).

[47] H.B. Callen and T.A. Welton, "Irreversibility and Generalized Noise." Phys. Rev. 83, 34-40 (1951).

[48] P. V. Yudin, R. Ahluwalia, and A. K. Tagantsev. Upper bounds for flexocoupling coefficients in ferroelectrics, Appl.Phys.Lett. **104**(8), 082913 (2014)

[49] M. J. Haun, Z.Q. Zhuang, E. Furman, S.J. Jang and L.E. Cross. "Thermodynamic theory of the lead zirconate-titanate solid solution system, part III: Curie constant and sixth-order polarization interaction dielectric stiffness coefficients." Ferroelectrics, Vol. 99, pp. 45-54 (1989).

[50] N.A. Pertsev, V.G. Kukhar, H. Kohlstedt, and R. Waser, "Phase diagrams and physical properties of single-domain epitaxial Pb (Zr 1− x Ti x) O 3 thin films." Phys. Rev. B **67**, 054107 (2003).

[51] M.J. Haun, E. Furman, S. J. Jang, H. A. McKinstry, and L. E. Cross. "Thermodynamic theory of PbTiO3." Journal of Applied Physics 62, no. 8: 3331-3338(1987).

[52] A. A. Kohutych, R. M. Yevych, S. I. Perechinskii, Y. M. Vysochanskii. Acoustic attenuation in ferroelectric $Sn_2P_2S_6$ crystals. Cent. Eur. J. Phys. **8**(6), 905 (2010)